Colloids and Surfaces B: Biointerfaces 66 (2008) 195–200

Contents lists available at ScienceDirect

Colloids and Surfaces B: Biointerfaces

journal homepage: www.elsevier.com/locate/colsurfb

Platinum nanoparticles have an activity similar to mitochondrial NADH:ubiquinone oxidoreductase

Keisuke Hikosaka [a], Juewon Kim [a], Masashi Kajita [a,b], Atsuhiro Kanayama [a,1], Yusei Miyamoto [a,*]

[a] Department of Integrated Biosciences, Graduate School of Frontier Sciences, University of Tokyo, Bioscience Building 402, 5-1-5 Kashiwanoha, Kashiwa, Chiba 277-8562, Japan
[b] APt Co. Ltd., 5-4-19 Kashiwanoha, TKVP Suite 201A, Kashiwa, Chiba 277-0082, Japan

ARTICLE INFO

Article history:
Received 25 March 2008
Received in revised form 10 June 2008
Accepted 13 June 2008
Available online 24 June 2008

Keywords:
Platinum nanoparticles
NADH oxidation
CoQ reduction
Mitochondria
Electron transport complex I

ABSTRACT

This study was designed to examine if platinum nanoparticles have an activity similar to mitochondrial complex I, NADH:ubiquinone oxidoreductase. Platinum nanoparticles were prepared by a citrate reduction of H_2PtCl_6 and protected by citrate itself and pectin (CP-Pt). Time- and dose-dependent decreases in NADH and a time-dependent increase in NAD^+ were observed in the presence of 50 μM CP-Pt; these observations were made using a spectrophotometric method in which the maximum absorption spectra at 340 and 260 nm were used for NADH and NAD^+, respectively. The required platinum concentration in CP-Pt to achieve a 50% oxidation of NADH for 3 h was approximately 20 μM, and this NADH oxidation did not require oxygen as an electron acceptor. We also verified NAD^+ formation using an NAD^+/NADH quantification kit. The absorption peak shift from 278 to 284 nm of 2,3-dimethoxy-5-methyl-6-(3-methyl-2-butenyl)-1,4-benzoquinone (CoQ_1) was observed by incubating CoQ_1 with CP-Pt in an aqueous buffer. A further analysis with HPLC revealed the reduction of CoQ_1 to CoQ_1H_2 by CP-Pt. As a whole, platinum nanoparticles have an NADH:ubiquinone oxidoreductase-like activity. This suggests that platinum nanoparticles are a potential medicinal substance for oxidative stress diseases with suppressed mitochondrial complex I.

1. Introduction

In the field of industrial chemistry, metal nanoparticles are used to create efficient catalysts [1–3]. Recently, the amount of research on their biological applications has increasing with the establishment of a new research field—bionanotechnology [4]. Gold nanoparticles coated with antibodies are used as nanomarkers; nanoparticles label antigens such that the antigens can be visually located and quantified under an electron microscope [5–7]. Because gold nanoparticles do not cause acute cytotoxicity [8], considerable attention has been directed to their use as a platform for targeted drug delivery [9–11]. Moreover, gold-biopolymer nanocomposites have been shown to be potential antioxidants that quench the hydroxyl radical [12–14].

Recently, our group showed that platinum nanoparticles prepared by citrate reduction have the ability to quench superoxide anion radical ($O_2^{-\bullet}$) and hydrogen peroxide (H_2O_2) [15]. Although the quenching mechanisms of $O_2^{-\bullet}$ have not been elucidated, some data indicate that they may be quenched by a catalytic redox reaction coupled with an electron transfer. Electron transfer by platinum nanoparticles has been demonstrated when they catalyze the reaction between hexacyanoferrate (III) ions and thiosulfate ions [16]. Moreover, some previous studies have shown that gold nanoparticles catalyze the oxidation of NADH to NAD^+ [17–20]. Complex I in the mitochondrial electron transport chain not only oxidizes NADH to NAD^+ but also reduces ubiquinone (CoQ) to ubiquinol ($CoQH_2$). If platinum nanoparticles can catalyze both reactions, they can mimic part of the enzymatic functions of complex I.

Mitochondrial electron transport complex I is composed of many subunits. Some of them are encoded at the genomic DNA in the nucleus, synthesized by the cytosolic polysome, and transported into the mitochondrial inner membrane [21]. Together with subunits translated in the mitochondria, complex I is assembled in the inner membrane [22]. Besides acting as a proton pump, this enzyme transports electrons from NADH to CoQ, thereby forming $CoQH_2$. $CoQH_2$ is also formed by mitochondrial complex II which transfers electrons from succinic acid. Subsequently, $CoQH_2$ is used as a substrate for complex III, and two electrons are transferred to cytochrome *c*. CoQ is also synthesized in the endoplasmic reticulum and Golgi membrane system. In these non-

* Corresponding author. Tel.: +81 4 7136 3628; fax: +81 4 7136 3630.
E-mail address: yusei74@k.u-tokyo.ac.jp (Y. Miyamoto).
[1] Present address: Department of Global Infectious Diseases and Tropical Medicine, National Defense Medical College, 3-2 Namiki, Tokorozawa, Saitama 359-8513, Japan.

0927-7765/$ – see front matter © 2008 Elsevier B.V. All rights reserved.
doi:10.1016/j.colsurfb.2008.06.008

mitochondrial membranes, $CoQH_2$ functions as an antioxidant which is essential for the defensive system against oxidative stress in tissues [23]. Nevertheless, the main biological function of CoQ seems to be as an electron carrier in the mitochondrial respiratory chain.

Recent studies have shown that reactive oxygen species (ROS) are thought to be involved in signal transduction pathways [24,25]. However, when they are overproduced, they take part in the onset and progression of many diseases. Mitochondria are the main tissue to generate ROS, especially $O_2^{-\bullet}$, which is generated as a by-product by the reaction of O_2 with a single electron leaked from mitochondrial electron transport complexes I and III [26]. Other ROS such as H_2O_2 and hydroxyl radical ($^\bullet OH$) can be formed from $O_2^{-\bullet}$; therefore, $O_2^{-\bullet}$ generated in mitochondria is a key ROS in the regulating the redox state in the body. In fact, oxidative stress, mitochondrial dysfunction, and suppression of mitochondrial electron transport complexes are involved in the pathogenesis of human diseases such as inflammation, atherosclerosis, neurodegenerative diseases, and hepatitis C [27–30]. Therefore, antioxidant therapy is one effective medical treatment for these diseases [31,32], with mitochondrial targeting of antioxidant agents expected to be more beneficial [33]. CoQ is an effective antioxidant for the medical treatment of neurodegenerative diseases [34].

In this paper, we assert that platinum nanoparticles have an activity that is similar to that of oxidizing NADH and reducing CoQ. This suggests that platinum nanoparticles can mimic part of the enzymatic functions of the complex I and indicates their possible use in medical treatments for oxidative stress diseases.

2. Experimental

2.1. Materials

Hydrogen hexachloroplatinate hexahydrate ($H_2PtCl_6{\cdot}6H_2O$), trisodium citrate dihydrate, NADH disodium salt, sodium borohydride, potassium hexacyanoferrate (III), HPLC-grade methanol, and distilled water were purchased from Wako Pure Chemical Industries, Ltd. (Osaka, Japan). Pectin was generously provided by Unitec Foods Co., Ltd. (Tokyo, Japan). 2,3-Dimethoxy-5-methyl-6-(3-methyl-2-butenyl)-1,4-benzoquinone (CoQ_1) was obtained from Sigma–Aldrich (St. Louis, MO, USA), and an NAD^+/NADH assay kit was purchased from BioAssay Systems, Inc. (Hayward, CA, USA). Amicon ultra centrifugal filter devices were from Millipore (Billerica, MA, USA). All other reagents were of the highest commercially available grades.

2.2. Preparation of platinum nanoparticles protected with citrate and pectin (CP-Pt)

CP-Pt was prepared by the citrate reduction of H_2PtCl_6 [4]. In a 100-ml eggplant-type flask, 43.8 ml of water and 4 ml of 16.6 mM H_2PtCl_6 were added. The mixture in the flask was stirred at 100 °C until reflux started. Then, 8.6 ml of 77.2 mM trisodium citrate dehydrate was injected into the reaction mixture and reflux was continued for additional 30 min. After the reaction mixture cooled to room temperature, 10 ml of 3.96 mg/ml pectin was added and the mixture was stirred for another hour. Citrate and pectin worked as protecting reagents. The reason why pectin was used as an additional protecting reagent was that platinum nanoparticle protected with citrate alone was not stable in isotonic solution such as 0.9% NaCl and pectin helped improve this instability as described previously [15]. For the sake of biological use of platinum nanoparticles in the near future, we used CP-Pt in this study.

2.3. Measurements

To confirm the reduction of platinum ions in $PtCl_6^{2-}$ and formation of CP-Pt, ultraviolet and visible (UV–vis) spectra were measured from 200 to 800 nm using an Ultrospec 6300 Pro spectrophotometer (GE Healthcare Bio-Science Corp., Uppsala, Sweden).

NADH and NAD^+ were quantified by their absorption spectra at 340 and 260 nm, respectively, using the spectrometer [17]. An NAD^+/NADH assay was also performed with the assay kit according to the manufacture's manual to estimate NAD^+ production. The method was based on the alcohol dehydrogenase cycling reaction in which a tetrazolium dye is reduced by NADH in the presence of phenazine methosulfate.

To investigate the chemical change of CP-Pt by NADH oxidation, UV–vis surface plasmon resonance absorption spectra of CP-Pt were measured from 200 to 800 nm after incubation with NADH. CP-Pt at 100 μM were incubated with 200 μM NADH in water at room temperature for 2 h. Subsequently, the incubated mixture was centrifuged by Amicon ultra centrifugal filter devices to remove NADH and NAD which impede the spectrum measurement. Then, samples were re-dispersed with the equal volume of water. This washing process was repeated 10 times. For a control experiment, we used CP-Pt subjected to 2 h incubation without NADH and following series of washing.

Reduction of CoQ_1 to CoQ_1H_2 was estimated by absorption peak shift, as previously described [35–37]. To clearly distinguish CoQ_1H_2 from CoQ_1, we used an HPLC system that was composed of a Waters 600 controller (Milford, MA, USA) with a Waters 996 Diode Array Detector and a 20 μl injection loop. The column and guard column used were 150 mm × 4.6 mm Supelcosil octadecylsilane LC-18-T (particle size: 3 μm, Supelco, Bellefonte, PA, USA) and 20 mm × 4 mm Discovery HS C18 (particle size: 3 μm, pore size: 120 Å, Supelco), respectively.

CoQ_1 and CoQ_1H_2 were separated at room temperature at a flow rate of 0.20 ml/min. The composition of one mobile phase was 80% methanol and 20% distilled water. To avoid reoxidation of CoQ_1H_2, water was degassed and all experiments were performed under an N_2 atmosphere. Column elution was monitored at 275 and 290 nm for CoQ_1 and CoQ_1H_2, respectively. To reduce and reoxidize CoQ_1, following solutions were prepared: 5 mM oxidized CoQ_1 in ethanol, 1 mM CP-Pt in water, 50 mM borohydride in water, and 50 mM ferricyanide in water. To create a reaction mixture using those solutions, the total volume was adjusted to 40 μl with 140 mM KCl and 10 mM HEPES/OH, pH 7.5 (HEPES/OH buffer). The final concentrations of CoQ_1, CP-Pt, borohydride and ferricyanide were 0.25, 0.25, 4, and 4 mM, respectively, in the reaction mixture. After the reaction was conducted in a microsyringe, half of the mixture (20 μl) was injected into the HPLC system. The concentration of CoQ_1H_2 was estimated from a standard curve of dimensions that were calculated using Millennium software 32 [38,39].

3. Results

3.1. Characterization of CP-Pt

CP-Pt was prepared by the citrate reduction of H_2PtCl_6. UV–vis spectra were recorded at $PtCl_6^{2-}$ and CP-Pt concentrations of 50 and 200 μM, respectively. After the reduction, the two absorption maxima of the $PtCl_6^{2-}$ spectrum (a sharp peak at 260 nm and a small broad peak around 370 nm) were not observed (Fig. 1). We judged that platinum ions were reduced to atoms. To confirm the dispersibility of CP-Pt and determine their diameter, electron micrographs were taken by H-7600 TEM manufactured by Hitachi

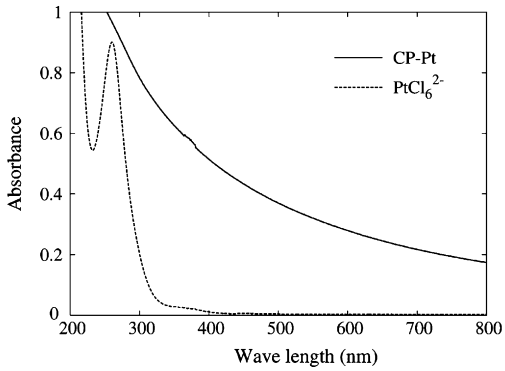

Fig. 1. UV–vis absorption spectra of platinum nanoparticles protected with citrate and pectin (CP-Pt) and aqueous hexachloroplatinate ($PtCl_6^{2-}$) from 200 to 800 nm. The concentrations of platinum as CP-Pt and as $PtCl_6^{2-}$ were 200 and 50 μM, respectively.

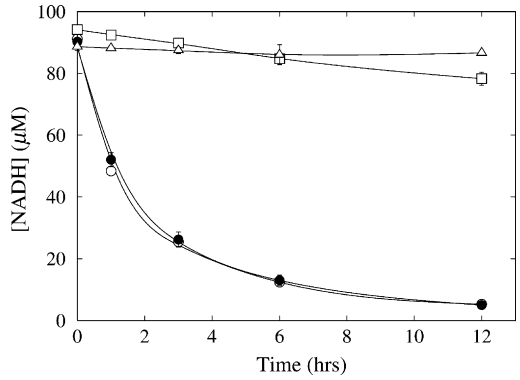

Fig. 3. Oxidation of NADH by platinum only. CP-Pt were incubated with NADH in water at room temperature for predetermined periods (open circle). The concentrations of platinum in CP-Pt and NADH were 50 and 100 μM, respectively, at the start of incubation. A similar experiment was performed under an N_2 atmosphere (closed circle). Auto-oxidation of NADH was monitored by incubating 100 μM NADH alone (open square). To examine whether the protecting reagents of CP-Pt oxidize NADH, citrate and pectin were incubated with NADH (open triangle). The concentrations of citrate and pectin were 10 mM and 0.60 mg/ml, respectively. The concentrations of NADH were calculated using the ε value of 6.22 mM^{-1} cm^{-1} [18]. Values represent means ± S.D. of five experiments. When not shown, deviations lie within the symbols.

Science Systems Ltd. (Tokyo, Japan). Their dispersibility and average diameter (data not shown) were similar to those reported previously [15].

3.2. Oxidation of NADH by CP-Pt

To determine if CP-Pt can oxidize NADH, 100 μM NADH was incubated with 50 μM CP-Pt for up to 12 h. The reaction was carried out at room temperature under a normoxic atmosphere. The absorbance decreased and increased with time at 340 and 260 nm, respectively (Fig. 2). This observation indicated that CP-Pt oxidized NADH to NAD^+. The NAD^+/NADH ratio after the 12 h incubation was 5.85 ± 1.23 (n = 3); about 85% of NADH was oxidized to NAD^+.

The time course of NADH oxidation by CP-Pt was then studied. With the addition of 50 μM CP-Pt, the concentration of NADH decreased in a time-dependent manner (Fig. 3). In 3 h, CP-Pt oxidized NADH by approximately 75%. When NADH was incubated with a mixture of protecting reagents, citrate and pectin, the time-dependent decrease of NADH was not observed; this observation indicated that the platinum in CP-Pt was the active agent for oxidizing NADH. When NADH alone was incubated, slight auto-oxidation was observed, as previously reported [40]. To examine if O_2 accepts electrons from NADH, NADH was incubated with CP-Pt under an N_2 atmosphere. Without O_2, CP-Pt still oxidized NADH.

When the concentration of platinum in CP-Pt was varied in the range of 0–100 μM, the oxidation of NADH for 3 h was dose-dependent (Fig. 4), and the CP-Pt concentration that could induce 50% oxidation of NADH was approximately 20 μM. To confirm that CP-Pt oxidized NADH to NAD^+, we measured the time course of the NAD^+/NADH concentration ratio using an NAD^+/NADH assay kit. This assay is highly specific for the measurement of NAD^+/NADH concentrations and ratios. The absorbance at 570 nm decreased by 30% for 2 h; consequently, about 70% of NADH was oxidized to NAD^+ (Fig. 5). The assay kit result was in good accordance with results determined by the absorbance peak shift from 340 to 260 nm.

After the oxidation of NADH, the UV–vis surface plasmon resonance absorption spectrum of CP-Pt was measured and exhibited the feature typical of platinum nanoparticles. The spectra of CP-Pt were identical before and after NADH oxidation, indicating that the NADH oxidation did not cause a significant chemical change of CP-Pt (Fig. 6).

3.3. Reduction of CoQ_1 by CP-Pt

The absorption spectra were monitored at 1 h after CP-Pt were mixed with CoQ_1 in the HEPES/OH buffer at room temperature. The maximum absorption peak shifted from 278 to 284 nm (Fig. 7), which suggests that the peak shift may be attributable to the reduction of CoQ_1 by CP-Pt. However, the maximum peaks we observed had a slight variance from those of oxidized and reduced CoQ_1, as previously reported [41,42].

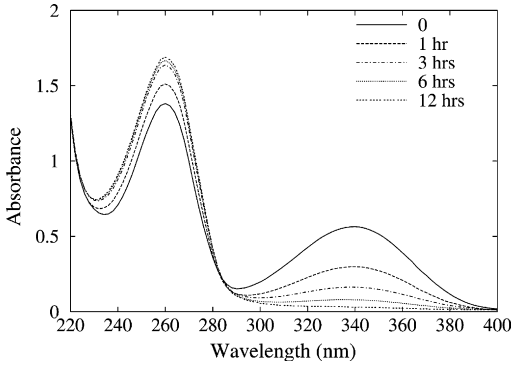

Fig. 2. Time-dependent change in absorption spectra. CP-Pt were incubated with NADH in water at room temperature for the indicated times. The concentrations of platinum in CP-Pt and NADH were 50 and 100 μM, respectively.

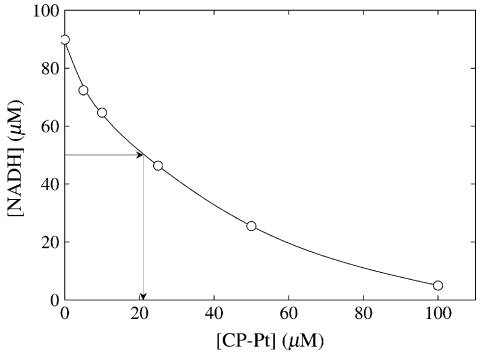

Fig. 4. Dose-dependent decrease in NADH. The absorption band at 340 nm was monitored for 3 h after CP-Pt were added to a 100-μM NADH solution. The concentration of platinum in CP-Pt was altered from 5 to 100 μM. Values represent means ± S.D. of five experiments. When not shown, deviations lie within the symbols.

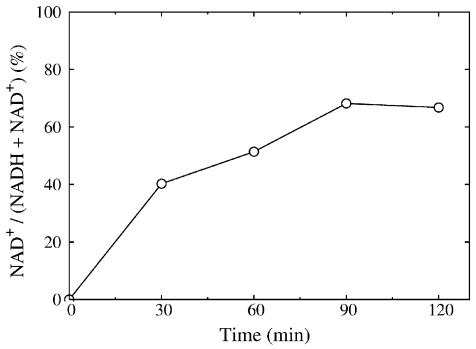

Fig. 5. Generation of NAD^+ by oxidation of NADH. The NAD^+/NADH concentrations and ratios were measured using an NAD^+/NADH assay kit. The absorbance at 570 nm was measured until 120 min after 5 μM CP-Pt were added to the 5 μM NADH solution. Values represent means ± S.D. of three experiments. When not shown, deviations lie within the symbols.

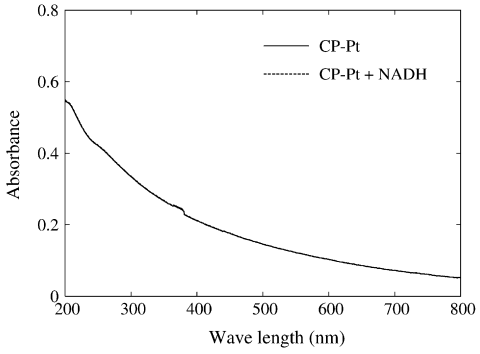

Fig. 6. UV–vis surface plasmon absorption spectra of CP-Pt after NADH oxidation. CP-Pt was incubated with NADH in water at room temperature for 2 h. The concentrations of platinum in CP-Pt and NADH were 100 μM and 200 μM, respectively. After 2 h reaction, the incubated mixture was centrifuged by Amicon Ultra centrifugal filter devices to remove NADH and NAD and then re-dispersed with the equal volume of water. This washing process was repeated 10 times. For control, we used CP-Pt subjected to 2 h incubation without NADH and following series of washing. The spectrum measurements were independently repeated three times. A representative set of spectra were shown.

We used HPLC to clearly separate CoQ_1 and CoQ_1H_2. Two microliters of 5 mM CoQ_1 was diluted with 38 μl of the HEPES/OH buffer, and half of the diluted solution (20 μl) was injected into the HPLC with the Supelcosil octadecylsilane LC-18-T column. A peak was detected with a retention time of approximately 21 min (Fig. 8A). To reduce CoQ_1, 4 mM borohydride was used. Immediately after mixing, 20 μl of the mixture was injected into the HPLC system,

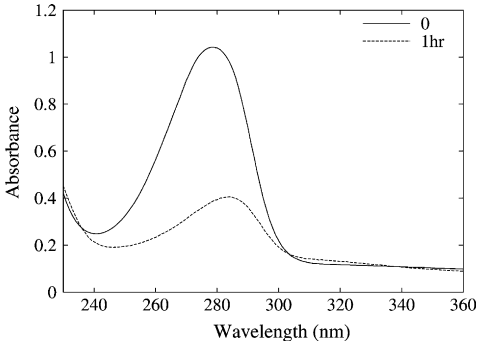

Fig. 7. The absorption change of CoQ_1. The CP-Pt were mixed with CoQ_1 in 140 mM KCl and 10 mM HEPES/OH, pH 7.5 (HEPES/OH buffer). Their final concentrations were 250 and 50 μM, respectively. The resultant mixture was incubated for 1 h at room temperature under an N_2 atmosphere.

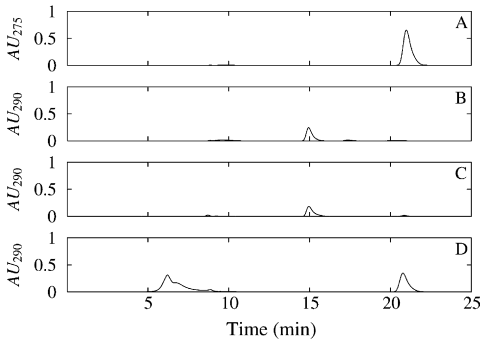

Fig. 8. HPLC analysis of CoQ_1. Twenty microliters of 0.25 mM CoQ_1 in the HEPES/OH buffer was injected into the HPLC (A). After a 1 h reduction with 4 mM borohydride, 20 μl of 0.25 mM CoQ_1 was injected (B). After a 1 h incubation with 0.25 mM CP-Pt at room temperature, 20 μl of the consequent mixture containing 0.25 mM CoQ_1 was injected (C). The concentration of ferricyanide was 4 mM, and the incubation time was 1 h (D). The 275 nm band is plotted in panel A, and the 290 nm band is plotted in panels (B–D). AU: absorption unit.

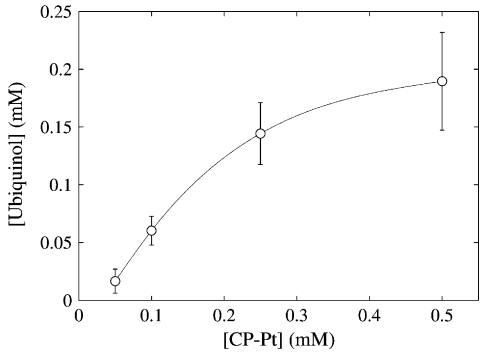

Fig. 9. Dose-dependent reduction of CoQ_1 by CP-Pt. CoQ_1 at 0.25 mM was incubated with 0.05, 0.1, 0.25, and 0.5 mM CP-Pt at room temperature for 15 min and detected at 290 nm with the HPLC system. The concentrations of reduced CoQ_1 were calculated as described in the Section 2. Values represent means ± S.D. of three experiments. When not shown, deviations lie within the symbols.

and CoQ_1H_2 was detected with a retention time of approximately 15 min (Fig. 8B). After a 1 h incubation of CoQ_1 with 0.25 mM CP-Pt, the mixture was injected. The peak in CoQ_1 was observed at the retention time of its reduced form (Fig. 8C), indicating that CP-Pt can reduce CoQ_1. To reoxidize CoQ_1, 4 mM ferricyanide was used in the mixture containing CP-Pt. The incubation time was 1 h and CoQ_1 was observed at the retention time of its oxidized form (Fig. 8D). The ferricyanide-derived peak was observed with retention time of approximately 6 min.

The dose dependency of CoQ_1 reduction was then studied. The concentration of platinum in CP-Pt was varied in the range of 0.05 to 0.5 mM, and a dose-dependent increase in CoQ_1H_2 was observed (Fig. 9). These results showed that CP-Pt reduced CoQ_1 in a dose-dependent manner.

4. Discussion

The decrease and increase in the absorption intensity at 340 and 260 nm, respectively, are interpreted as the oxidation of NADH to NAD^+ because the bands at 340 and 260 nm are from the n–π* transition of the dihydronicotinamide part and π–π* transition of the adenine ring, respectively, as described in a previous study of gold nanoparticles [17]. A similar peak shift was observed with CP-Pt in this study (Fig. 9), indicating that CP-Pt has the same activity as that of oxidizing NADH to NAD^+. We also detected NAD^+ with a more definitive method; we used an NAD^+/NADH quantification

kit, which indirectly found NAD^+ by detecting the NAD^+ cycling enzyme. This kit enabled us to measure NAD^+ formed by the CP-Pt oxidation of NADH (Fig. 5). We estimated the concentration of platinum atoms in CP-Pt from its ion concentration at the beginning of the nanoparticle preparation because platinum ions were hardly detected after the citrate reduction (Fig. 1). Because platinum nanoparticles do not have a specific absorption peak, we could not calculate the concentration of platinum nanoparticles. Considering the face-centered cubic structure of gold nanoparticles, these nanoparticles whose diameter is 15 nm consist of approximately 1.0×10^5 gold atoms [17]. According to previous results, the concentration of gold nanoparticles needed for 50% oxidation of NADH (IC_{50}) was approximately 0.5 nM; from this nanoparticle concentration, a gold atom concentration is estimated to be 50 μM. The IC_{50} of platinum atoms was 20 μM (Fig. 3). Although these values are in relatively good agreement, oxidizing NADH is slower with platinum than with gold because 1-h incubation with CP-Pt was required before NADH oxidation could be detected.

When NADH is oxidized to NAD^+, H^+ and $2e^-$ are released. Therefore, CP-Pt has to take care of $2e^-$, too. It is well known that upon ultraviolet irradiation, platinum nanoparticle-loaded photocatalyst TiO_2 decomposes water to evolve hydrogen ($2H_2O + 2e^- \rightarrow 2OH^- + H_2\uparrow$) [43]. Platinum nanoparticles help function for electron transfer to water. Because a chemical change of CP-Pt was not observed after the oxidation of NADH (Fig. 6), we speculate that besides the oxidation of NADH, CP-Pt may transfer (accept and release, as discussed afterward) electrons to water, decompose it and generate hydrogen.

From the spectrum changes, we assumed that CoQ_1 was reduced by CP-Pt (Fig. 7). The alternation of the maximum absorption peak in water and absolute ethanol were previously discussed in detail [44]. From their study, the maximum peak of oxidized CoQ_1 in a tris-acetate buffer was 278 nm. We measured the maximum peak of the oxidized form in a HEPES/OH buffer and found the value to be 279 nm. A 1-nm peak shift seems to be due to the difference of media. We could not find information about the maximum peak of reduced CoQ_1 in theirs and other researches' papers. When considering the height of these absorption peaks, the oxidized form is higher than that of the reduced form due to the difference in their extinction coefficients. The millimolar extinction coefficient difference ($\Delta\varepsilon$) between oxidized and reduced CoQ_{10} was obtained to be 12.5 [35]. In our study, the $\Delta\varepsilon$ for CoQ_1 calculated between the absorption at 279 and 284 nm was 12.7, slightly high from $\Delta\varepsilon$ 12.3 [45]. Therefore, we believe that CoQ_1 was not reduced completely by CP-Pt in 1 h.

To quantify oxidized and reduced CoQ, HPLC is often employed by utilizing the affinity difference to the octadecylsilane column [46]. For CoQ_1 separation, 70% methanol and 30% ethanol are usually used as a mobile phase solution [47]. We observed that when using this mobile phase solution, CP-Pt aggregated and precipitated. We developed a mobile phase consisting of 80% methanol and 20% distilled water to maintain a good dispersion of CP-Pt. We measured the maximum peak of oxidized and reduced CoQ_1 in 80% methanol media and the values were 275 and 290 nm, respectively (data not shown). With this mobile phase solution in the HPLC system, the retention times of oxidized and reduced CoQ_1 were 21 and 15 min, respectively, in the HPLC system we used (Fig. 8). These data show that CP-Pt can reduce CoQ_1. Ferricyanide was used as an oxidant according to a previous report [48], and this reagent completely reoxidized the reduced CoQ_1 (Fig. 8D). Due to ferricyanide oxidizing the reduced CoQ_1, the reduction of CoQ_1 by CP-Pt is related to the structural changes of quinone to quinol.

Since the CP-Pt consisted of platinum, citrate, and pectin, platinum ions, free citrate, and free pectin might have oxidized NADH and reduced CoQ_1. We did not examine effects of platinum ions because platinum ions were reduced nearly 100% after citrate reduction (Fig. 1). In the current study, we confirmed that a protecting reagent, either citrate or pectin, did not oxidize NADH (Fig. 3). The reduction of CoQ_1 was not observed in the presence of either protecting reagents (data not shown). We believe that the activity of oxidizing NADH and reducing CoQ_1 is attributable to the platinum atoms in CP-Pt.

The complex I of mitochondrial electron transport is located at the mitochondrial inner membrane. It functions in the matrix to oxidize NADH and in the inner membrane to transfer electrons to CoQ. Therefore, platinum nanoparticles possibly substitute the complex I if we can deliver them to the proper mitochondrial locations: the matrix and inner membrane. Recent reports on electron localization in platinum and palladium nanoparticles demonstrated that electrons are located at the interface between the nanoparticles and protecting reagents. This phenomenon is a consequence of contributions from both the quantum-size effect and the charge-transfer from the metal nanoparticle core [49,50]. If platinum nanoparticles are ready to accept and release electrons due to their electron surface location, platinum nanoparticles can separately mediate two reactions: oxidation of NADH in the matrix and reduction of CoQ in the inner membrane. In other words, even though platinum nanoparticles do not directly transfer electrons from NADH to CoQ, they can supply NAD^+ to the tricarboxylic acid (TCA) cycle and reduced CoQ to complex III. Therefore, platinum nanoparticles can potentially mimic the enzymatic activity of complex I, though currently, we do not know if they can function as a proton pump, which mitochondrial complex I can perform.

5. Conclusions

The mitochondrial respiratory chain, especially at complexes I and III, is thought of as a primary site of ROS generation. In some oxidative stress diseases such as Parkinson's disease [51], excessive ROS generation is responsible to pathogenesis due to the suppression of complex I. Platinum nanoparticles serve dual functions as mitochondrial complex I to lower ROS generation and as SOD/catalase mimetics to scavenge generated excessive ROS. Our recent *in vivo* study has revealed the lifespan extension of *Caenorhabditis elegans* by platinum nanoparticles [52]. If we can deliver platinum nanoparticles to proper sites in the mitochondria, they seem to be useful for the medical treatment of oxidative stress diseases.

References

[1] J.D. Aiken III, R.G. Finke, J. Mol. Catal. A: Chem. 145 (1999) 1.
[2] A. Roucoux, J. Schulz, H. Patin, Chem. Rev. 102 (2002) 3757.
[3] J.S. Bradley, G. Schmid, in: G. Schmid (Ed.), Nanoparticles, Wiley-VCH, Weinheim, 2004, pp. 186–199.
[4] W.R.J. Glomm, Disp. Sci. Technol. 26 (2005) 389.
[5] K. Mannweiler, H. Hohenberg, W. Bohn, G. Rutter, J. Microsc. 126 (1982) 145.
[6] F.T. Bosman, Histochem. J. 15 (1983) 189.
[7] G.M. Hodges, Arch. Histol. Cytol. 55 (1992) 27.
[8] E.E. Connor, J. Mwamuka, A. Gole, C.J. Murphy, M.D. Wyatt, Small 1 (2005) 325.
[9] J.M. Bergen, H.A. von Recum, T.T. Goodman, A.P. Massey, S.H. Pun, Macromol. Biosci. 6 (2006) 506.
[10] R.K. Visaria, R.J. Griffin, B.W. Williams, E.S. Ebbini, G.F. Paciotti, C.W. Song, J.C. Bischof, Mol. Cancer. Ther. 5 (2006) 1014.
[11] G.F. Paciotti, D.G.I. Kingston, L. Tamarkin, Drug. Dev. Res. 67 (2006) 47.
[12] K. Esumi, N. Takei, T. Yoshimura, Colloids Surf. B: Biointerfaces 32 (2003) 117.
[13] K. Esumi, H. Houdatsu, T. Yoshimura, Langmuir 20 (2004) 2536.
[14] S. Akiyama, T. Yoshimura, K. Esumi, J. Jpn. Soc. Colour Mater. 78 (2005) 112.
[15] M. Kajita, K. Hikosaka, M. Iitsuk, A. Kanayama, N. Toshima, Y. Miyamoto, Free Radic. Res. 41 (2007) 615.
[16] R. Narayanan, M.A. El-Sayed, J. Phys. Chem. B. 107 (2003) 12416.
[17] X. Huang, I.H. El-Sayed, X. Yi, M.A. El-Sayed, J. Photochem. Photobiol. B: Biol. 81 (2005) 76.
[18] V.S. Kulikova, Kinet. Catal. 46 (2005) 399.
[19] C.R. Raj, B.K. Jena, Chem. Commun. 2005 (2005) 2005.

[20] B.K. Jena, C.R. Raj, Anal. Chem. 78 (2006) 6332.
[21] J. Smeitink, L. van den Heuvel, Am. J. Hum. Genet. 64 (1999) 1505.
[22] R. Vogel, L. Nijtmans, C. Ugalde, L. van den Heuvel, J. Smeitink, Curr. Opin. Neurol. 17 (2004) 179.
[23] F. Aberg, E.L. Appelkvist, G. Dallner, L. Ernster, Arch. Biochem. Biophys. 295 (1992) 230.
[24] T. Finkel, Curr. Opin. Cell. Biol. 10 (1998) 248.
[25] J.S. Stamler, S. Lamas, F.C. Fang, Cell 106 (2001) 675.
[26] J.F. Turrens, J. Physiol. 552 (2003) 335.
[27] M. Valko, D. Leibfritz, J. Moncol, M.T.D. Cronin, M. Mazur, J. Telser, Int. J. Biochem. Cell. Biol. 39 (2007) 44.
[28] M.P. Mattson, Nat. Rev. Mol. Cell. Biol. 1 (2000) 120.
[29] A.C. Rego, C.R. Oliveria, Neurochem. Res. 28 (2003) 1563.
[30] T. Wang, S.A. Weinman, J. Gastroenterol. Hepatol. 21 (2006) S34.
[31] V. Di Matteo, E. Esposito, Curr. Drug Targets 2 (2003) 92.
[32] A. Melhem, M. Stern, O. Shibolet, E. Israeli, Z. Ackerman, O. Pappo, N. Hemed, M. Rowe, H. Ohama, G. Zabrecky, R. Cohen, Y. Ilan, J. Clin. Gastroenterol. 39 (2005) 737.
[33] M.F. Beal, Ann. Neurol. 58 (2005) 495.
[34] M.F. Beal, J. Bioenerg. Biomembr. 36 (2004) 381.
[35] F.L. Crane, R. Barr, Methods Enzymol. 18 (1971) 137.
[36] F.L. Crane, Y. Hatefi, R.L. Lester, C. Widner, Biochim. Biophys. Acta 25 (1957) 220.
[37] C.-A. Yu, L. Gu, Y. Lin, L. Yu, Biochemistry 24 (1985) 3897.
[38] D.V. Ratnam, V. Bhardwaj, M.N.V. Ravi Kumar, Talanta 70 (2006) 387.
[39] E.A. Mazzio, R.R. Reams, K.F.A. Soliman, Brain Res. 1004 (2004) 29.
[40] F. Petrat, T. Bramey, M. Kirsch, U. Kerkweg, H. de Groot, Free Radic. Res. 40 (2006) 857.
[41] S. Chen, R.J. Guillory, J. Biol. Chem. 252 (1977) 8990.
[42] A. Mordente, G.E. Martorana, S.A. Santini, G.A. Miggiano, T. Petitti, B. Giardina, M. Battino, G.P. Littarru, Clin. Invest. 71 (1993) S92.
[43] S. Tabata, H. Nishida, Y. Masaki, K. Tabata, Catal. Lett. 34 (1995) 245.
[44] M.D. Esposti, E. Bertoli, G. Parenti-Castelli, R. Fato, S. Mascarello, G. Lenaz, Arch. Biochem. Biophys. 210 (1981) 21.
[45] K. Inaba, K. Ito, EMBO J. 21 (2002) 2646.
[46] J. Lagendijk, J.B. Ubbink, W.J. Hayward Vermaak, J. Lipid Res. 37 (1996) 67.
[47] M. Jemiota-Rzeminska, D. Latowski, K. Strzalka, Chem. Phys. Lipids. 110 (2001) 85.
[48] S.H. Audi, H. Zhao, R.D. Bongard, N. Hogg, N.J. Kettenhofen, B. Kalyanaraman, C.A. Dawson, M.P. Merker, Free Radic. Biol. Med. 34 (2003) 892.
[49] W. Tu, K. Takai, K. Fukui, A. Miyazaki, T. Enoki, J. Phys. Chem. B 107 (2003) 10134.
[50] W. Tu, K. Fukui, A. Miyazaki, T. Enoki, J. Phys. Chem. B 110 (2006) 20895.
[51] L. Tretter, I. Sipos, V. Adam-Vizi, Neurochem. Res. 29 (2004) 569.
[52] J. Kim, M. Takahashi, T. Shimizu, T. Shirasawa, M. Kajita, A. Kanayama, Y. Miyamoto, Mech. Ageing Dev. 129 (2008) 322.